Cumulative radiation exposure from medical imaging and associated lifetime cancer risk in children with osteogenesis imperfecta

Thorby-Lister, Amy; Hoegler, Wolfgang; Hodgson, Kirsten; Crabtree, Nicola; Uday, Suma; Nightingale, Peter; Shaw, Nick; Saraff, Vrinda

DOI:
10.1016/j.bone.2018.06.021

Document Version
Peer reviewed version

Citation for published version (Harvard):
Thorby-Lister, A, Hoegler, W, Hodgson, K, Crabtree, N, Uday, S, Nightingale, P, Shaw, N & Saraff, V 2019, 'Cumulative radiation exposure from medical imaging and associated lifetime cancer risk in children with osteogenesis imperfecta', *Bone*, vol. 114, pp. 252-256. https://doi.org/10.1016/j.bone.2018.06.021

Title:

Cumulative radiation exposure from medical imaging and associated lifetime cancer risk in children with osteogenesis imperfecta.

Authors:

Amy Thorby-Lister[a], Wolfgang Högler[a,b], Kirsten Hodgson[c], Nicola Crabtree[a], Peter Nightingale[d], Nick Shaw[a,b], Vrinda Saraff[a]

Affiliations:

a) Department of Endocrinology and Diabetes, Birmingham Women's and Children's Hospital, Steelhouse Lane, Birmingham, B4 6NH, UK

b) Institute of Metabolism and Systems Research, University of Birmingham, IBR Tower, Level 2, College of Medical and Dental Sciences, Edgbaston, Birmingham, B15 2TT, UK

c) Radiation Physics and Protection Services, University Hospitals Birmingham NHS Foundation Trust, 63 Melchett Road, Kings Norton Business Centre, Birmingham, B30 3HP, UK

d) Institute of Translational Medicine, Heritage Building, Mindelsohn Way, Edgbaston, Birmingham, B15 2TH, UK

Corresponding author:

Dr Vrinda Saraff

Department of Endocrinology and Diabetes

Birmingham Women's and Children's Hospital

Steelhouse Lane, Birmingham, B4 6NH, United Kingdom

Fax: 0121 333 8191

Email: vrinda.saraff@nhs.net

Abstract:

Objectives:

To estimate the cumulative effective dose of radiation (E) and additional lifetime attributable risk (LAR) of cancer from ionizing radiation in children with osteogenesis imperfecta (OI), who require frequent imaging for fractures and bone densitometry (DXA) surveillance. Also, to evaluate the pattern of long bone fractures.

Methods:

We reviewed all imaging (x-rays, DXA and computed tomography [CT]) conducted in a cohort of children with OI with a minimum observation period of 5 years. For each image, E was estimated using age-dependent local data, and LAR of cancer was extrapolated. LAR and fracture data were compared among children with mild, moderate and severe OI. LAR was allocated to cancer risk categories, and the moderate risk group (1 in 1,000 to 1 in 100) was evaluated further.

Results:

Results from 106 children with OI (50% females, 5747 images) are presented, with a median (range) observation period of 11.7 (5.2-15.6) years. CT accounted for 0.8% of total imaging procedures but contributed to 66% of total E. The overall LAR of cancer was minimal, averaging an additional 8.8 cases per 100,000 exposed patients (0.8-403). LAR was significantly lower in children with mild OI compared to those with moderate (p=0.006) and severe OI (p=0.001). All patients with a moderate LAR of cancer (n=8) had undergone CT scans and 88%

had scoliosis or vertebral fractures. The cohort experienced 412 long bone fractures, with the most common site being the femur (26.5%). OI severity correlated positively with long bone fracture rates ($p<0.001$).

Conclusions:

When compared to baseline LAR of cancer (50%) the additional cancer risk from ionizing radiation imaging in our paediatric OI cohort was small (0.0088%). To reduce additional cancer risk, we recommend replacing spinal x-rays with vertebral fracture assessments on DXA and exercising caution with CT imaging.

Keywords:

Osteogenesis imperfecta, cumulative radiation exposure, lifetime cancer risk, x-rays, fractures.

Funding sources:

This research did not receive any specific grant from funding agencies in the public, commercial, or not-for-profit sectors.

1. Introduction:

Osteogenesis imperfecta (OI) is a heterogeneous, inheritable bone fragility disorder, caused by defects in the production or processing of type I collagen. Affected children experience low impact fractures, poor fracture healing, decreased linear bone growth and bony deformities [1].

Fractures in general are common in children, with peak incidence rates at 14 years in boys and 11 years in girls [2]. In a cohort of Danish subjects with OI, the highest fracture rate was also in childhood (0-19 years of age) with peak incidence rates between 0-5 years and 10-15 years in boys, and 0-10 years in girls [3]. Fracture frequency is also influenced by OI phenotype; children with mild OI have an annual incidence rate of less than 1, moderate OI of 3, and severe OI of greater than 3 fractures [4].

Given their high fracture risk, children with OI require multiple x-rays for investigation of suspected fractures, as well as serial follow-up x-rays to assess fracture healing. They also require regular monitoring of bone densitometry and radiological assessment for vertebral fractures and spinal deformities, which further adds to their cumulative radiation exposure [5]. The effective dose of radiation (E) from multiple radiological examinations results in an additional lifetime cancer risk. For each unit (Sievert) of radiation exposure, the risk of cancer is highest for girls aged 0 to 9 years [5]. Cancer risk is also dependent on the body site exposed to the radiation [6]. Cancer following exposure to high-dose radiation is usually seen within 3-5 years for leukaemia and beyond 10-15 years for solid tumors [7]. Repetitive radiation exposure at an early age may result in a significant lifetime cancer risk in children with OI. In contrast to other

childhood chronic illnesses [8-13], no studies to date have assessed cancer risk from radiation exposure in children with OI.

1.1 Aims:

1. To estimate cumulative E and additional lifetime attributable risk (LAR) of cancer from diagnostic and surveillance imaging performed on a cohort of children with OI. To compare E and LAR across age groups, OI phenotypes, sex and with respect to family history of OI.
2. To compare the number of long bone fractures by site, age and OI phenotype.
3. To evaluate if family history of OI or OI phenotype affects the proportion of fracture-positive images in children presenting with an injury.

2. Methods:

2.1 Study design and patient selection:

This is a retrospective observational cohort study. Due to the nature of the study, ethics approval was not required. The cohort included all patients managed at Birmingham Children's Hospital, UK, with a clinical diagnosis of OI. Patients were selected from the hospital OI database. To ensure the follow up period was representative we chose a minimum observation period of 5 years.

2.2 Patient-specific data collection:

The following demographic data was collected for each patient; sex, age, type of OI based on clinical phenotype, genetic confirmation of OI (if available) and family history of OI in a first-degree relative. Each patient was classified as either

mild, moderate or severe phenotype based on the updated Sillence classification [4].

Each patient's imaging procedures that involved the use of ionizing radiation (x-ray, dual-energy x-ray absorptiometry (DXA) and computed tomography (CT)) were reviewed on the institution's 'Picture Archiving and Communication System' (PACS) from birth or 2003 (installation of the PACS system) until December 2016. Therefore, the observation period differed in the cohort, ranging between 5 -15 years. For each imaging procedure, the following was recorded; age of patient at scan, type of scan (x-ray, DXA or CT), region of body scanned, reason for scan, presence of a new fracture (as described in radiologist's report), site of fracture and estimated E in milliSievert (mSv).

2.3 Fracture-positive rate:

'Reason for the scan' was documented in five categories; investigation for injury with a fracture reported (fracture-positive) or without (fracture-negative), ongoing monitoring of fracture healing, surveillance imaging (e.g. for scoliosis), and no reason identified. We then calculated the rate of fracture-positive x-rays relative to all x-rays taken for investigation of injury.

2.4 Estimation of effective radiation dose:

Age-specific E for each image type was estimated with data collected from our institution using the PCXMC x-ray dosimetry program (A Monte Carlo Program for Calculating Patient Doses in Medical X-ray Examinations, Version 2.0, 2008, STUK, Finland) or the ImPACT CT Dosimetry program (CT patient Dosimetry Calculator, Version 1.0.4, 2011, ImPACT, London, UK). If this data was not

available then standard data (i.e.: not age-specific) was used, from HPA-CRCE-012 Report Appendix A (E_{103}) [14]. For DXA scans, E was determined with reference to the manufacturer's specifications (Lunar enCORE iDXA, GE Medical Systems Lunar, Madison, USA).

2.5 Estimation of lifetime attributable risk of cancer:

For each patient cumulative E was calculated by summing E, in two exposure age groups (0-9 and 10-19 years) and five different body sites (head, neck, chest, abdomen and pelvis). To calculate LAR, cumulative E was multiplied by an age, body site and sex-specific risk coefficients as per HPA-CRCE-028 Report, Table 29, page 56 [6]. These values were then summed to give the total LAR for that individual's period of observation. Each patient's LAR was then extrapolated to an observation period of 18 years to allow results to be comparable. LAR data was then allocated to a cancer risk category as described in HPA-CRCE-028 Report, page 49-50 [6].

2.6 Statistical analysis:

The above calculations used Microsoft Office Excel 2010 (Microsoft Corporation, Redmond, WA) and data was statistically analyzed by a qualified statistician using SPSS (SPSS Statistics for Windows, Version 22.0, Armonk, NY:IBM Corp). To compare LAR in male and female patients a Mann-Whitney test was used. Kruskal-Wallis and Dunn's tests were used to compare the three OI phenotypes with respect to LAR, cumulative E per year, number of fracture-positive x-rays per year and the fracture-positive rate. To assess the impact of age on radiation exposure each patient's cumulative E data was split into five age groups: 0-2, 2-5,

5-9, 9-14 and 14-19 years, and a Jonckheere-Terpstra test was used to compare E in each group. Impact of family history on cumulative E, LAR and fracture-positive rate was assessed using a Mann-Whitney test. A Jonckheere-Terpstra test was used to compare long bone fracture rate between OI phenotypes and Fisher's exact tests to evaluate fracture site and age groups.

3. Results:

A total of 197 children with OI were identified from the hospital database. Forty-five children were under five years of age and 46 were managed jointly with peripheral hospitals (all images of whom were not available for review) and hence they were excluded. The final study cohort therefore comprised 106 patients, 53 males and 53 females. Phenotypically, 74 patients were considered to have mild OI, 22 moderate and 10 severe. Further details about the cohort are summarized in Table 1.

Table 1: Characteristics of the study cohort: OI phenotype, sex, family history of OI, observation period and age [median (range)].

OI phenotype	Male	Female	Family history	Observation period (years)	Age at inclusion (years)
Mild (n=74)	39	35	51 (69%)	11.2 (5.2-14.2)	2.47 (0.00-15.10)
Moderate (n=22)	10	12	13 (59%)	14.0 (5.7-15.4)	2.95 (0.01-11.20)
Severe (n=10)	4	6	6 (60%)	11.0 (6.5-15.6)	0.01 (0.00-2.23)

The types of OI included in this study were Type I (n=72), Type III (n=6), Type IV (n=17), Type V (n=2), Type IX (n=3), Type XI (n=1), Type XIII (n=2) and Type XIV (n=3).

Over the median (range) observation period of 11.7 years (5.2 – 15.6) a total of 5747 images using ionizing radiation were performed, averaging 3.8 images per patient per year. Of the total imaging procedures, 91.6% were x-rays, 7.6% DXA, and 0.8% were CT. Across the cohort, CT contributed to 66% of cumulative E, while x-ray and DXA were 31% and 3% respectively (Figure 1).

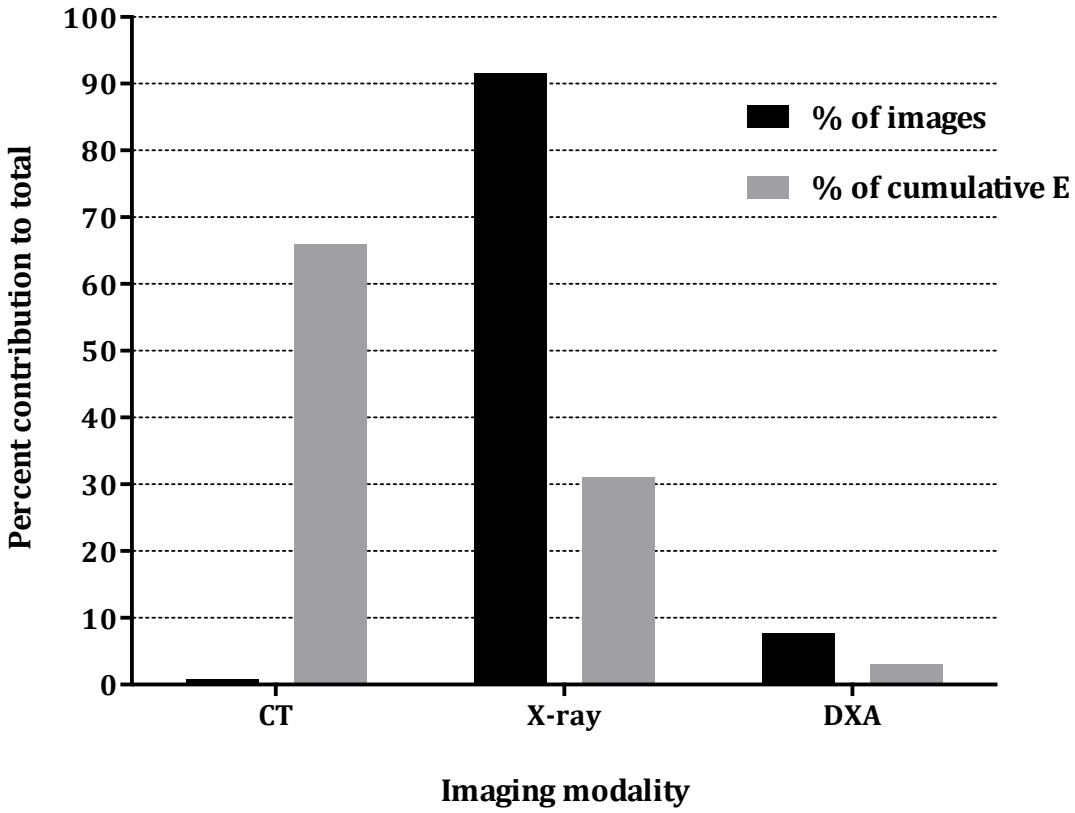

Figure 1: Contribution of each imaging modality to total number of imaging procedures and cumulative effective dose of radiation (E).

3.1 Cumulative effective radiation doses:

The median cumulative E across the cohort was 0.45 mSv (0.02 - 14.99), or 0.04 mSv per year. Cumulative E per year was lower in children with mild OI compared to moderate ($p = 0.006$) and severe OI ($p = 0.001$), but was not different between moderate and severe phenotypes ($p = 0.715$) (Table 2). When examining cumulative E by age group there was a significant trend for increased E with age ($p \leq 0.001$). The 9-14 year age group had the highest E mean at 0.169 mSv/year (SD 0.33) [range 0-1.6] and the 2-5 year age group had the lowest E at 0.089 mSv/year (SD 0.29) [range 0-1.94].

Table 2: Number of images, cumulative E and LAR (predicted number of cancer cases per 100,000 exposed) for each OI phenotype [median (IQR 25-75)].

OI phenotype	Total number of images	Images per year	Total cumulative E (mSv)	Cumulative E per year (mSv/year)	LAR of cancer
Mild	33 (17-47)	3.1 (1.9–5.0)	0.323 (0.123-1.061)	0.029 *Ψ (0.012 - 0.086)	5.5 *Ψ (2.3-14.3)
Moderate	57 (33-91)	5.4 (2.7–8.2)	0.887 (0.479 – 2.382)	0.069 (0.040 – 0.228)	13 (8.3-55.7)
Severe	138 (76-192)	9.8 (5.9–22.9)	1.821 (0.834 – 8.127)	0.137 (0.059 – 0.685)	27 (10.8-118.3)

* $p \leq 0.01$ when compared to moderate

$^{\Psi}p=0.001$ when compared to severe

3.2 Predicted LAR of cancer:

The median additional LAR of cancer across the whole cohort was 8.8 cases per 100,000 exposed patients (0.0088%). LAR did not differ between sexes (p=0.997). However, LAR was significantly lower in mild OI compared to

moderate (p=0.01) and severe OI (p=0.001), but did not differ between moderate and severe OI (p=0.644) (Table 2, Figure 2).

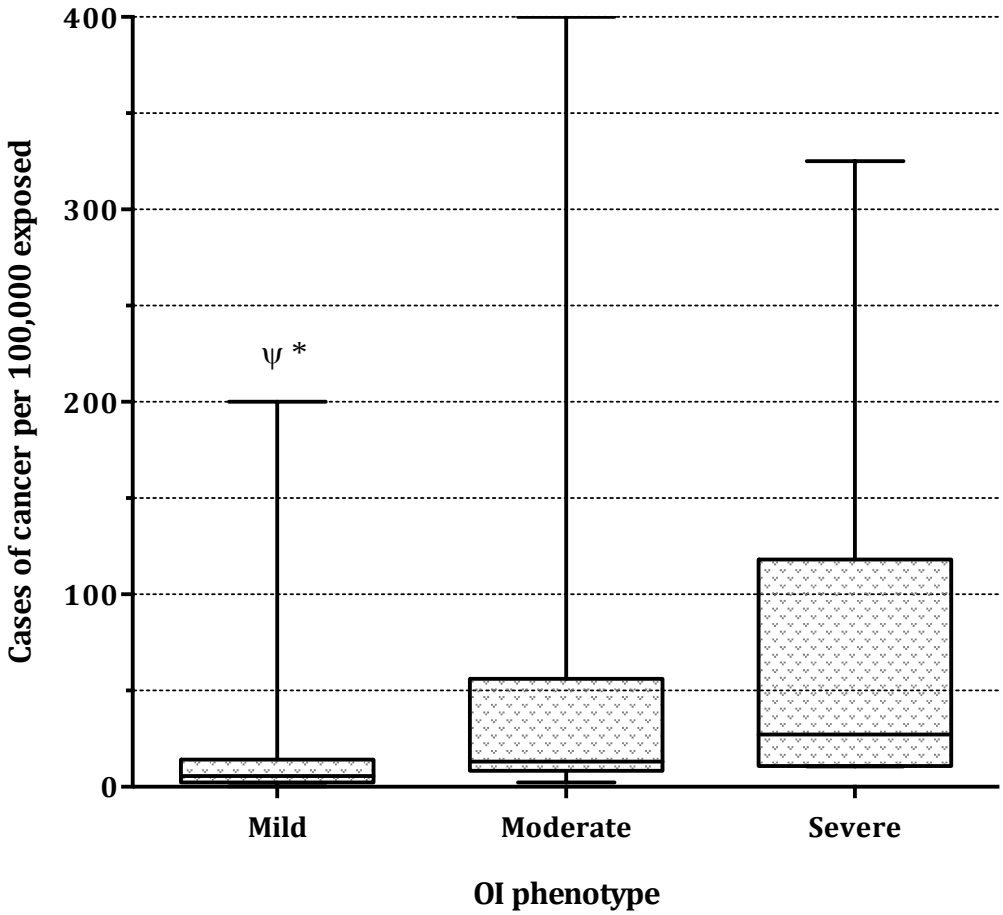

* p ≤ 0.01 when compared to moderate

ψ p = 0.001 when compared to severe

Figure 2: Number of predicted cases of cancer per 100,000 exposed patients, secondary to radiation from medical imaging (median, IQR 25 & 75 and range).

Figure 3 shows LAR of cancer by risk category, noting that half of the cohort falls into 'very low risk' (1 case in 100,000 to 1 in 10,000). Patients with severe OI are

either categorized as 'low' (1 in 10,000 to 1 in 1,000) or 'moderate' risk (1 in 1,000 to 1 in 100).

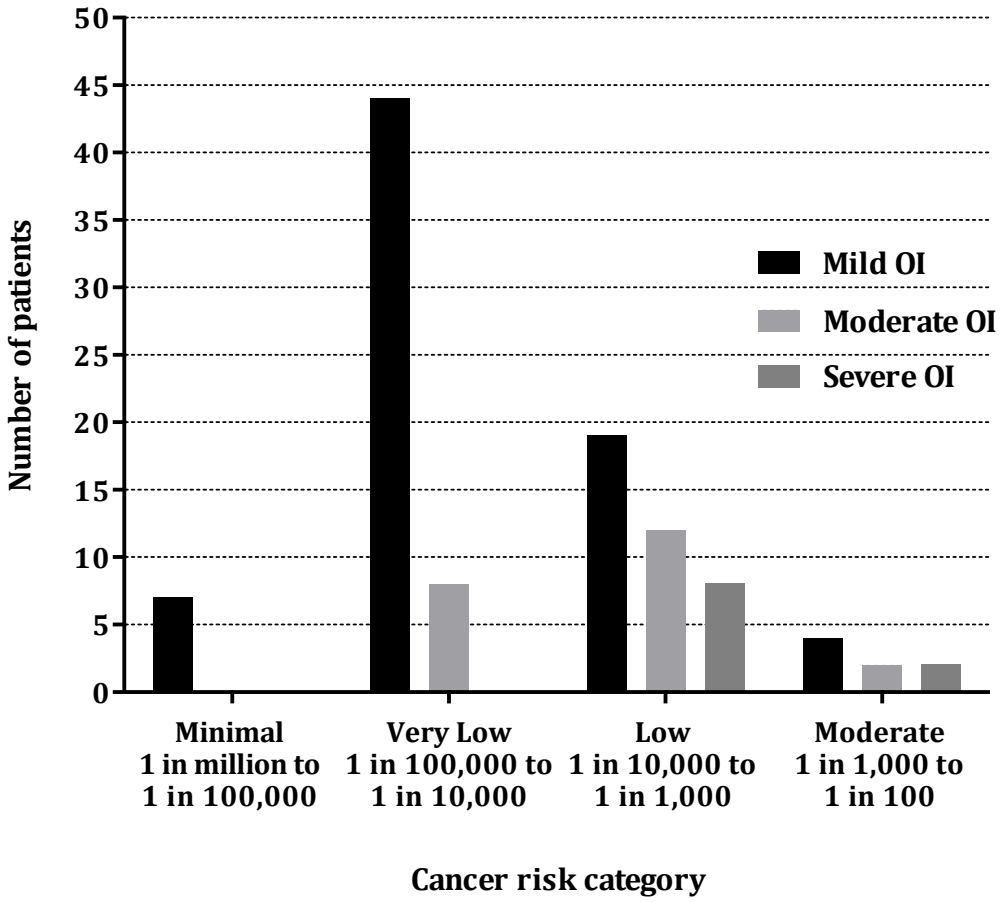

Figure 3: Lifetime attributable risk (LAR) of cancer by risk category and OI phenotype

Further characterisation of the moderate risk patients (Table 4), demonstrates the contribution of CT scans and repeated spinal x-rays to overall LAR. Patients in the moderate risk group had more spinal x-rays (median 0.904/yr) when compared to patients in the low and very low risk groups (0.503/yr and 0.155/yr respectively).

Table 4: Characteristics of patients in the moderate risk of cancer category (1 in 1,000 to 1 in 100).

Patient	OI phenotype	Number of spinal x-rays	Number of CT scans	Vertebral fractures/ scoliosis	Observation period (years)	LAR of cancer
1	Mild	17	1	Yes	8	1 in 925
2	Mild	15	6	Yes	12	1 in 662
3	Mild	0	3	No	6	1 in 495
4	Mild	8	1	No*	14	1 in 841
5	Moderate	13	2	Yes	7	1 in 478
6	Moderate	11	3	Yes	7	1 in 248
7	Severe	9**	2	Yes	10	1 in 307
8	Severe	21	2	Yes	8	1 in 343

* Note: Patient 4 has a history of spondylolisthesis

**Note: Patient 7 had 16 pelvic x-rays (due to bilateral femoral neck fractures)

3.3 Fracture patterns:

The cohort experienced 412 long bone fractures; the most common bone fractured was the femur (26.5%, $p < 0.001$). OI severity correlated positively with long bone fracture rates ($p<0.001$), with the median annual fracture rate (range) for mild OI at 0.20 (0-1.00), moderate 0.28 (0-2.43) and severe 0.80 (0-3.22). Categorized by age group, the most common long bone fractured was the femur (45% of patients) in 0-2 year olds, tibia (30%) in 2-5, radius (23%) in 5-9 and

femur in both 9-14 (31%) and 14-19 year olds (46%). 73% of the cohort had radiographic evidence of at least one vertebral fracture.

3.4 Fracture-positive rate:

The rate of fracture-positive imaging was 60%, i.e. for every 10 images taken for investigation of an injury 6 would identify a fracture. Both the rate of fracture-positive imaging and the number of fracture-positive images per year were not different between OI phenotypes (p=0.654 and 0.051, respectively). This may be due to the small number of patients with severe OI, as clinically a difference would be expected.

3.5 Family history of OI:

There was no significant difference in cumulative E or LAR (p = 0.371 and 0.254 respectively) between patients with and without an affected first-degree family member. A sub-analysis of these two groups by OI phenotype also showed no significant difference in cumulative E (mild p=0.678, moderate p=0.117 and severe p=0.136). Of note, a family history of OI did not influence the rate of fracture-positive imaging (p=0.764).

4. Discussion:

This is the first study to assess cumulative E and LAR of cancer in a cohort of paediatric patients with OI. Here we demonstrate that the typical OI patient in our cohort underwent an average of 3.8 imaging procedures per year using ionizing radiation. As expected, the number of imaging procedures and LAR

correlated with OI severity. Radiation awareness is important, since each mSv of radiation encountered during childhood has a 2-5 fold increase in the risk of developing cancer when compared to the same dose of radiation received during adulthood [6]. However, since x-ray was the most common imaging modality in our cohort, the cumulative E and LAR appears less than for other chronic childhood illnesses where high-radiation procedures are more common (such as congenital heart disease[8]).

There are only a few other studies that used similar methods of calculating cancer risk, the most relevant examines a cohort of patients with complex congenital heart disease [8]. Their median cumulative E (2.7mSv) and estimated LAR (65 cases per 100,000 exposed) was much higher than in our cohort. However, cardiac catheterization contributed to 60% of the total E. Similar to our cohort, the severity of the disease correlated with the LAR of cancer (1677 cases per 100,000 exposed in the cardiac transplant group). The difference in cumulative E and LAR between the moderate and severe OI phenotypes did not reach significance. We hypothesize this was due to the small group of patients with severe OI (n=10), equally it could also be explained by the younger age at study inclusion and hence the observation period not covering the whole of adolescence (9-14 years) when cumulative E was found to be at it's highest.

In the moderate risk of cancer group, all patients had at least one CT scan and most (88%) required repeated spinal x-rays. Although CT scans were not performed frequently (0.8% of imaging events) they contributed to a large portion (66%) of the total exposure in our cohort. This highlights the importance

of radiation protection principles (justification, optimization, dose limits) and should encourage clinicians to consider alternatives to CT where possible [15].

Yearly cumulative E peaked at 9-14 years of age, which is consistent with the period of highest fracture incidence in the general childhood population in the UK [2]. As expected long bone fracture rates showed a significant upward trend with increasing severity of OI. The most common fracture sites were femur, tibia and radius which is similar to other published data [3,16].

We had speculated that a positive family of OI, which assumes a better understanding of the condition and less parental anxiety, would lead to fewer presentations with minor injuries and hence higher rates of fracture-positive imaging. However, this hypothesis was not supported by our data. Interestingly, patients with severe OI also had no change in their fracture-positive rate, although this may again be secondary to the small sample size (n=10).

The strengths of this study include a large rare-disease cohort, a long period of observation (median 11.7 years) and the method of calculating cumulative E by reviewing each individual image. Radiation exposure from routine examinations is not standardized in paediatrics, however we used institution-specific age-dependent E data whenever available, and this added to the accuracy of calculating cumulative E. We also used published age, body site and sex-specific risk coefficients to calculate LAR, as each of these factors impact lifetime cancer risk.

A limitation of this study is the small sample size in the severe OI phenotype group (n=10). We did not have the required information to calculate patient-specific E doses, although by using age-dependent E this provided a good estimation. We recognize that to compare LAR, data was extrapolated to 18 years, and this may have led to a slight overestimation, most notably in the patients with short observation periods and high cumulative E doses (such as Patient 3, Table 4). However, the overall trend of increasing LAR with OI severity mirrors the increase seen in cumulative E, which is un-extrapolated data.

4.1 Conclusions:

In conclusion, given that the lifetime risk of developing cancer in the UK is 50% [17], the predicted additional risk of cancer from medical imaging in our cohort was minimal. However we identified a high-risk group (those with vertebral fractures, scoliosis or severe OI) that would benefit from a reduction in radiation exposure. Replacing spinal x-rays with Vertebral Fracture Assessment (VFA) using DXA can considerably lower radiation exposure but give similar clinical information [18]. We suggest using VFA as a screening tool for vertebral fractures and for routine surveillance of vertebral height (such as vertebral remodeling while on bisphosphonate therapy) [19]. Considering alternative forms of imaging, such as MRI, DXA or EOS imaging, in an attempt to avoid CT is also imperative [20]. Improvements in the medical management of patients with OI have resulted in a longer life expectancy, therefore the cumulative E from medical imaging we report becomes more relevant.

References:

[1] A. Bregou Bourgeois, B. Aubry-Rozier, L. Bonafé, L. Laurent-Applegate, D.P. Pioletti, P.-Y. Zambelli, Osteogenesis imperfecta: from diagnosis and multidisciplinary treatment to future perspectives, Swiss Med Wkly. 146 (2016) w14322. doi:10.4414/smw.2016.14322.

[2] R.J. Moon, N.C. Harvey, E.M. Curtis, F. de Vries, T. van Staa, C. Cooper, Ethnic and geographic variations in the epidemiology of childhood fractures in the United Kingdom, Bone. 85 (2016) 9–14. doi:10.1016/j.bone.2016.01.015.

[3] L. Folkestad, J.D. Hald, A.K. Ersbøll, J. Gram, A.P. Hermann, B. Langdahl, et al., Fracture Rates and Fracture Sites in Patients With Osteogenesis Imperfecta: A Nationwide Register-Based Cohort Study, Journal of Bone and Mineral Research. 32 (2017) 125–134. doi:10.1002/jbmr.2920.

[4] F.S. Van Dijk, D.O. Sillence, Osteogenesis imperfecta: Clinical diagnosis, nomenclature and severity assessment, American Journal of Medical Genetics Part A. 164 (2014) 1470–1481. doi:10.1002/ajmg.a.36545.

[5] P. Trejo, F. Rauch, Osteogenesis imperfecta in children and adolescents-new developments in diagnosis and treatment, Osteoporos Int. 27 (2016) 3427–3437. doi:10.1007/s00198-016-3723-3.

[6] B.F. Wall, R. Haylock, J. Jansen, M.C. Hillier, D. Hart, P.C. Shrimpton, Radiation risks from medical X-ray examinations as a function of the age and sex of the patient, Health Protection Agency Centre for Radiation, Chemical and Environmental Hazards. (2011).

[7] R.A. Kleinerman, Cancer risks following diagnostic and therapeutic

radiation exposure in children, Pediatr Radiol. 36 (2006) 121–125. doi:10.1007/s00247-006-0191-5.

[8] J.N. Johnson, C. Hornik, J.S. Li, D.K. Benjamin, T. Yoshizumi, R.E. Reiman, et al., Cumulative Radiation Exposure and Cancer Risk Estimation in Children with Heart Disease, Circulation. 130 (2014) CIRCULATIONAHA.113.005425–167. doi:10.1161/CIRCULATIONAHA.113.005425.

[9] M. Morin Doody, J.E. Lonstein, M. Stovall, D.G. Hacker, N. Luckyanov, C.E. Land, et al., Breast Cancer Mortality After Diagnostic Radiography: Findings From the U.S. Scoliosis Cohort Study, Spine. 25 (2000) 2052.

[10] A.B. Miller, G.R. Howe, G.J. Sherman, J.P. Lindsay, M.J. Yaffe, P.J. Dinner, et al., Mortality from Breast Cancer after Irradiation during Fluoroscopic Examinations in Patients Being Treated for Tuberculosis, N Engl J Med. 321 (2010) 1285–1289. doi:10.1056/NEJM198911093211902.

[11] B. Modan, L. Keinan, T. Blumstein, S. Sadetzki, Cancer following cardiac catheterization in childhood, Int J Epidemiol. 29 (2000) 424–428. doi:10.1093/ije/29.3.424.

[12] X.O. Shu, Y.T. Gao, L.A. Brinton, M.S. Linet, J.T. Tu, W. Zheng, et al., A population-based case-control study of childhood leukemia in Shanghai, Cancer. 62 (1988) 635–644. doi:10.1002/1097-0142(19880801)62:3<635::AID-CNCR2820620332>3.0.CO;2-3.

[13] X.O. Shu, J.D. Potter, M.S. Linet, R.K. Severson, D. Han, J.H. Kersey, et al., Diagnostic X-rays and ultrasound exposure and risk of childhood acute lymphoblastic leukemia by immunophenotype, Cancer Epidemiol. Biomarkers Prev. 11 (2002) 177–185.

[14] D. Hart, B.F. Wall, M.C. Hillier, P.C. Shrimpton, Frequency and collective dose for medical and dental X-ray examinations in the UK, 2008, Health Protection Agency. (2010).

[15] K.E. Applegate, N.G. Cost, Image Gently: a campaign to reduce children“s and adolescents” risk for cancer during adulthood, J Adolesc Health. 52 (2013) S93–7. doi:10.1016/j.jadohealth.2013.03.006.

[16] K.V. Peddada, B.T. Sullivan, A. Margalit, P.D. Sponseller, Fracture Patterns Differ Between Osteogenesis Imperfecta and Routine Pediatric Fractures, J Pediatr Orthop. 38 (2018) e207–e212. doi:10.1097/BPO.0000000000001137.

[17] A.S. Ahmad, N. Ormiston-Smith, P.D. Sasieni, Trends in the lifetime risk of developing cancer in Great Britain: comparison of risk for those born from 1930 to 1960, Br. J. Cancer. 112 (2015) 943–947. doi:10.1038/bjc.2014.606.

[18] J. Damilakis, J.E. Adams, G. Guglielmi, T.M. Link, Radiation exposure in X-ray-based imaging techniques used in osteoporosis, Eur Radiol. 20 (2010) 2707–2714. doi:10.1007/s00330-010-1845-0.

[19] N.J. Crabtree, S. Chapman, W. Högler, K. Hodgson, D. Chapman, N. Bebbington, et al., Vertebral fractures assessment in children: Evaluation of DXA imaging versus conventional spine radiography, Bone. 97 (2017) 168–174. doi:10.1016/j.bone.2017.01.006.

[20] P.H. Pedersen, A.G. Petersen, S.E. Østgaard, T. Tvedebrink, S.P. Eiskjær, EOS® Micro-Dose Protocol: First Full-Spine Radiation Dose Measurements in Anthropomorphic Phantoms and Comparisons with EOS Standard-Dose and Conventional Digital Radiology (CR), Spine.

1 (2018) 1. doi:10.1097/BRS.0000000000002696.

2